Critical Care

RESEARCH

Open Access

Structural and functional alteration of the gut microbiomes in ICU staff: a cross-sectional analysis

Bing Xie[1,2†], Chenyang Dong[1,2†], Xin Zhao[1,2†], Lianlian Qu[3†], Yongling Lv[4†], Hong Liu[1,2], Jiaxin Xu[1,2], Zhizhong Yu[1,2], Hexiao Shen[4*], You Shang[1*], Xing Zhao[1*] and Jiancheng Zhang[1,2*]

Abstract

Background 16S rRNA sequencing has revealed structural alterations in the gut microbiomes of medical workers, particularly those working in intensive care unit (ICU). This study aims to further compare the taxonomic and functional characteristics of gut microbiomes between ICU staff and non-medical individuals using metagenomic sequencing.

Methods A prospective cross-sectional cohort study was conducted, fecal samples from 39 individuals in each group—ICU staff and non-medical subjects were analyzed using metagenomic sequencing. PERMANOVA (using the adonis function) was employed to analyze the genus-level profiles and assess the impact of individual parameters on the gut microbiome. Multiple databases were utilized to annotate and compare the functional differences in gut microbiomes between the two groups.

Results We observed that ICU staff exhibited a significant decrease in gut microbiome diversity, characterized by a marked decline in Actinobacteria and a substantial increase in Bacteroides and Bacteroidaceae. CAZy annotation revealed a notable increase in carbohydrate-active enzymes within the ICU staff cohort. Kyoto Encyclopedia of Genes and Genomes (KEGG) analysis further indicated an elevated risk of endocrine and metabolic disorders, along with enhanced glycan biosynthesis and metabolism. Additionally, KEGG pathway enrichment analysis highlighted significant enrichment in cancer-related pathways. Analysis using the Virulence Factor Database (VFDB) showed a higher abundance of virulence factors associated with immune modulation, invasion, and antimicrobial activity/competitive advantage among ICU staff. Notably, no discernible difference in the presence of antibiotic resistance genes within the gut microbiomes was observed between the two groups. Importantly, all aforementioned differences demonstrated clear gender disparities.

†Contributed equally: Bing Xie, Chenyang Dong, Xin Zhao, Lianlian Qu, and Yongling Lv.

*Correspondence:
Hexiao Shen
hexiaoshen@hubu.edu.cn
You shang
you_shanghust@163.com
Xing Zhao
zhaoxing@hust.edu.cn
Jiancheng Zhang
zhjcheng1@126.com
Full list of author information is available at the end of the article

Conclusions Our findings indicated that ICU staff exhibited a reduction in gut microbiome diversity which was associated with an increase in virulence factors and carbohydrate-active enzymes, as well as with a heightened susceptibility to endocrine and metabolic diseases and cancers.

Keywords Metagenomic sequencing, Gut microbiome, Intensive care unit, Microbial dysbiosis, Functional annotation

Introduction

Intensive care unit (ICU) patients are at an elevated risk of intestinal dysbiosis due to the use of medications such as broad-spectrum antibiotics, proton pump inhibitors, opioids, and catecholamines, as well as underlying diseases, poor nutrition, mechanical ventilation, and the ICU environment [1, 2]. Notably, broad-spectrum antibiotics indiscriminately eliminate both pathogenic and commensal gut microbiomes, facilitating the rapid colonization by drug-resistant pathogens [2, 3]. This dysbiosis could lead to reduced short-chain fatty acid (SCFA) production, increased infection susceptibility, immune dysregulation, cytokine storms, worsened organ dysfunction, and higher mortality rates [4, 5].

In addition to intestinal dysbiosis in ICU patients, a prior study employing 16S rRNA sequencing revealed significant deviations in gut microbiome diversity among full-time medical workers, accompanied by alterations in microbial composition and functionality. Notably, both short-term and long-term medical workers exhibited increased abundances of taxa such as *Clostridiaceae*, *Clostridium*, *Dialister*, and *Desulfovibrio*, alongside a decreased abundance of Bacteroides compared to non-medical individuals. Additionally, the department in which medical staff worked (ICU versus non-ICU) had a marked influence on their gut microbiomes. Furthermore, the study suggested a potential correlation between the gut microbiomes of medical workers and the microbiota present in hospital environments [6].

Pathogenic bacteria, particularly multidrug-resistant organisms (MDROs), primarily disseminate within healthcare facilities through direct contact [7]. Frontline medical staff in ICUs continually interact with critically ill patients harboring MDROs and are exposed to the unique ICU environment for extended periods. This elevated risk of contact and exposure may lead to the integration of numerous pathogenic microorganisms and their associated antibiotic resistance genes (ARGs) into the gut microbiomes of ICU healthcare professionals, who could then act as carriers. Moreover, medical staff colonized with MDROs may become novel infection sources, potentially triggering outbreaks within a defined scope. Therefore, it is crucial to investigate whether the gut microbiomes of ICU staff harbor ARGs.

However, traditional molecular techniques, such as PCR amplification of 16S rRNA genes, provide limited taxonomic resolution and do not adequately address microbial functionality or the complex interactions within the microbiome. In contrast, metagenomics enables direct sequencing of the entire metagenomic DNA, thereby overcoming limitations associated with PCR, including primer restrictions and amplification biases. Moreover, metagenomics offers comprehensive taxonomic classifications and quantitative insights into functional and metabolic profiles [8]. However, the functional alterations and ARG carriage within the gut microbiomes of ICU staff remain poorly understood. Metagenomic sequencing offers a comprehensive approach to elucidate both the compositional and functional characteristics of gut microbiota, as well as the prevalence of ARGs. Therefore, there is an urgent need for metagenomic analysis to systematically compare the taxonomic and functional profiles, along with ARG carriage of gut microbiomes, between ICU staff and non-medical individuals. Previous studies have shown that human gut microbiota differ by gender [9, 10], influencing disease susceptibility in men versus women, including conditions such as obesity, diabetes, gout, inflammatory bowel disease, Alzheimer's disease, autism, depression, and various autoimmune diseases [9]. Gender-based subgroup analysis is also warranted.

In this study, we employed metagenomic sequencing to analyze fecal samples collected from ICU staff and healthy non-medical controls. The primary objectives were to detect variations in gene expression within their gut microbiomes, compare microbial community structures, and annotate functional differences using multiple databases, including Gene Ontology (GO), Kyoto Encyclopedia of Genes and Genomes (KEGG), evolutionary genealogy of genes: Non-supervised Orthologous Groups (eggNOG), carbohydrate-active enZymes (CAZy), virulence factor database (VFDB), and comprehensive antibiotic resistance database (CARD). Additionally, we investigated the relationship between ARGs and microbial communities.

Materials and methods

Ethics statement

This study protocol received approval from the Ethics Committee of Union Hospital, Tongji Medical College, Huazhong University of Science and Technology

(Permission Permission No. 0468). The study has been registered on ClinicalTrials with the identifier NCT06524765, on the date of 07/11/2024. Written informed consent was obtained from each participant.

Participants and sample collection

We strictly screened all doctors and nurses in the adult mixed medical-surgical ICU of Union Hospital, Tongji Medical College, Huazhong University of Science and Technology according to the inclusion and exclusion criteria, and a total of 39 full-time medical staff were recruited. For the past five years, all included ICU staff have been scheduled to undertake one 8-h night shift every 3–5 days. They are granted approximately two rest days each week, with the remaining days assigned to 10-h day shifts. The inclusion criteria for ICU staff encompassed (1) individuals aged 25–40 years, irrespective of their ethnicity or gender; (2) doctors and nurses directly engaged in the treatment and care of ICU patients, possessing a minimum of five years of ICU experience, and having been absent from frontline duties for less than 1 consecutive month.

The non-medical control group included 39 healthy individuals who had not worked at or visited hospitals for a year prior to participating in this study. The inclusion criteria for the non-medical control included (1) individuals aged 25–40 years, irrespective of their ethnicity or gender; (2) individuals who do not reside with a healthcare professional employed in an ICU. The inclusion criteria for the non-medical control group encompassed (1) individuals aged between 25 and 40 years, irrespective of their ethnicity or gender; (2) persons who do not cohabit with a healthcare professional employed in an ICU.

The exclusion criteria encompassed: (1) active gastrointestinal infections or chronic gastrointestinal disorders; (2) substantial dietary modifications or significant weight fluctuations exceeding 5 kg within a 3-month period; (3) use of antibiotics, proton pump inhibitors, prebiotics, and probiotics (including yogurt) in the last 4 weeks; (4) alcohol consumption within the past week; (5) recent treatment with high-risk immunosuppressive or cytotoxic medications, such as medium to high doses of glucocorticoids (20 mg/day or more) for a duration exceeding 4 weeks; (6) a history of major gastrointestinal surgery; (7) chronic conditions that may affect gut microbiomes; (8) congenital or acquired immunodeficiency disorders; (9) unwillingness to provide information on dietary habits, physical activity, and other lifestyle factors that could influence microbiome composition; (10) pregnancy or breastfeeding.

Demographics and baseline characteristics, including age, gender, body mass index (BMI), ethnic group, education level, smoking status, comorbid conditions, Bristol stool (form) scale (BSFS), exercise frequency, daily sleep duration, dietary preferences, mealtime regularity, history of digestive diseases, presence of foul-smelling flatulence or stools, severe halitosis, and pollen-food allergy, were collected.

Fecal sample collection and DNA extraction

Fecal samples were collected from each participant within thirty minutes of defecation and promptly stored at −80 ℃. All sample collections were completed in the morning and within one week following study enrollment. Genomic DNA was extracted using the HiPure Stool DNA Mini Kit (Magen) according to the manufacturer's protocol. The DNA concentration was quantified using a Qubit fluorometer (Thermo Fisher Scientific), and the integrity of the extracted genomic DNA was assessed via 1.5% agarose gel electrophoresis. Quality control criteria included: DNA concentration ≥ 20 ng/μL, volume ≥ 20 μL, total amount ≥ 400 ng, with good or slightly degraded DNA integrity; or DNA concentration between 5 and 20 ng/μL, volume ≥ 20 μL, total amount between 100 and 400 ng, with good or slightly degraded DNA integrity.

Metagenomic sequencing

All samples were sequenced on the Illumina NovaSeq 6000 platform. RawReads were processed using Trimmomatic (version 0.39) for adapter trimming and quality filtering with parameters: LEADING:3, TRAILING:3, SLIDINGWINDOW:50:20, MINLEN:100. KneadData (version 0.10.0) was utilized to remove contaminant sequences originating from the host, resulting in Clean Reads. The CleanReads were assembled into Contigs using MEGAHIT (version 1.2.9), with Contigs shorter than 500 bp being discarded. Prodigal (version 2.6.3) was utilized to predict coding DNA sequences (CDS) on the contigs, discarding those shorter than 100 bp. CD-HIT (version 4.8.1) was applied to cluster the genes obtained from each sample and remove redundancy, with a threshold of coverage > 90% and identity > 95%. Salmon (version 1.10.1) was utilized to calculate the transcripts per million (TPM) values for each gene in each sample. Using TPM values as relative abundances, species abundance and functional abundance were subsequently derived by summing the TPM values.

Taxonomic profiling

Bacteria, archaea, fungi, and viral sequences were extracted from the NR database (dated 2022–07–16) to form a sub-database. This sub-database was then aligned against a non-redundant gene set using DIAMOND (version 2.0.11) [11] with the following parameters: –evalue 0.00001 –max-target-seqs 10. Based on the top 10

sequences ranked by Score, the taxonomy classification of each gene was determined using the lowest common ancestor (LCA) method implemented in MEGAN software (version 6.24.20) [12]. The abundance of each taxonomic group was calculated by summing the abundances of genes assigned to that group. Additionally, Linear discriminant analysis effect size (LefSe) (version 1.1.2) analysis was performed on features with a relative abundance exceeding 0.0001.

α-diversity and β-diversity

A-diversity (within-sample diversity) was estimated based on the gene profiles of each sample according to the Simpson index, Shannon index and Chao 1 index. β-diversity (between-sample diversity) was assessed using principal component analysis (PCA), principal coordinates analysis (PCoA), and non-metric multidimensional scaling (NMDS). These analyses were conducted using the Vegan R package. β-diversity metrics were calculated using Bray–Curtis dissimilarity and Jaccard distance. To detect statistically significant differences in β diversity between groups, a permutational multivariate analysis of variance (PERMANOVA) and analysis of similarity (ANOSIM) were employed.

Functional annotation of non-redundant genes

Using DIAMOND (version 2.0.11) [11], the non-redundant gene set was aligned against the Non-Redundant Protein Sequence Database (NR) sub-database, with an E-value threshold of $< 1e^{-5}$. The top hit was selected, and the corresponding GO number was retrieved based on the accession number. To obtain KEGG Orthology (KO) annotations for non-redundant genes, KofamScan [13] was employed with a threshold E-value $< 1e^{-4}$, selecting the KO annotation with the smallest e-value as the definitive annotation. Additionally, enrichment analysis of KEGG pathways was conducted based on significantly different KOs identified by metagenomeSeq [14]. EggNOG annotations were obtained for non-redundant genes using eggNOG-mapper (version 2.1.9) [15]. To identify antibiotic resistance genes within the non-redundant gene set, the CARD 2023 database was utilized [16]. The CARD ontology encompasses three categories: antimicrobial resistance (AMR) Gene Family, Drug Class, and Resistance Mechanism. The Resistance Gene Identifier (RGI) tool (version 6.0.1) of the CARD database, which employs the DIAMOND algorithm, was used to annotate antibiotic resistance genes, providing annotations for these three categories and subsequently calculating their relative abundance. Carbohydrate-active enzymes in the non-redundant gene set were identified using dbcan3 [17], referencing the CAZy database. dbcan3 employs a combination of three methods for identification: (1) searching the dbcan-specific HMM database using HMMER, (2) searching the CAZyme sequence database using DIAMOND, and (3) eCAMI. Annotations were retained when at least two of these three methods provided consistent CAZyme annotations. BLASTP (Protein–Protein BLAST 2.5.0+) was used to align the non-redundant genes against the Virulence Factor Database (VFDB) [18], applying an E-value threshold of $< 1e^{-5}$, with the top hit serving as the annotation result. The total abundance of non-redundant genes within each functional category was summed to represent the abundance of that functional category.

Statistical analysis

All statistical analyses were conducted using GraphPad Prism, version 8 (GraphPad Software, La Jolla, CA, USA). Demographic information of participants was analyzed using two-tailed Mann–Whitney *U* test, Chi-squared test, or Fisher's exact test as appropriate. The two-tailed Mann–Whitney *U* test was employed to assess the significance of the metagenomic data. To evaluate the effect of host characteristics on the gut microbiome, PERMANOVA was performed at the amplicon sequence variant (ASV) level using the adonis function from the vegan R-package. Statistical significance was set at $P < 0.05$.

Results

Participant characteristics

This study included 78 healthy Chinese participants, comprising 39 ICU staff and 39 non-medical controls. The basic characteristics of all the participants are summarized in Table 1. ICU staff and non-medical controls exhibited similar characteristics in terms of age, gender, BMI, ethnic group, education level, smoking status, comorbidities, BSFS, exercise frequency, daily sleep duration, mealtime regularity, history of digestive diseases, presence of foul-smelling flatulence or stools, severe halitosis, and pollen-food allergy. Both groups had a male proportion of 41%. Notably, non-medical controls reported more frequent exercise within the past year and more regular meal times compared to ICU staff.

Distinct gut microbial diversity and structure in ICU staff

We conducted PERMANOVA on the gut microbial composition across the entire cohort to examine whether ICU medical work status correlated with the overall community structure. Stratification of ICU staff and non-medical controls accounted for 33.8% of the gut microbiota variance (*adonis* $P = 0.001$). This effect size exceeded those of other collected confounding factors (Table 2), indicating that ICU medical work status was a primary determinant of gut microbiome composition in our study population.

Table 1 Demographics and baseline characteristics

	Total (n = 78)	ICU staff (n = 39)	Non-medical controls (n = 39)	*P* value
Working time in ICU, median (IQR), years	9 (6–13)	9 (6–13)	–	–
Age, median (IQR), years	30 (26–34)	31 (28–34)	39 (26–30)	0.0632
Gender				
Male	32 (41.0)	16 (41.0)	16 (41.0)	–
Female		23 (59.0)	23 (59.0)	
BMI, median (IQR), kg/m^2	22.8 (20.7–24.6)	22.7 (21.0–24.2)	23.4 (20.3–24.7)	0.8057
Ethnic group				
Han	74 (93.7)	39 (100)	35 (89.7)	0.1153
Others	4 (10.3)	0 (0)	4 (10.3)	
Education level				
≤ High school	1 (1.3)	0 (0)	1 (2.6)	> 0.9999
University or college	63 (80.8)	33 (84.6)	30 (76.9)	0.3887
Master or doctor	14 (17.9)	6 (15.4)	8 (20.5)	0.5551
Smoking status	5 (6.4)	3 (7.7)	2 (5.1)	> 0.9999
Comorbidities				
Neuropsychiatric disorder	3 (3.8)	2 (5.1)	1 (2.6)	> 0.9999
Skin disease	5 (6.4)	3 (7.7)	2 (5.1)	> 0.9999
Tumor	2 (2.6)	1 (2.6)	1 (2.6)	–
Chronic kidney disease	1 (1.3)	1 (2.6)	0 (0)	> 0.9999
Upper respiratory tract disease	1 (1.3)	0 (0)	1 (2.6)	> 0.9999
Metabolic disease	5 (6.4)	4 (10.3)	1 (2.6)	0.3584
BSFS				
Type 1	1 (1.3)	0 (0)	1 (2.6)	> 0.9999
Type 2	5 (6.4)	2 (5.1)	3 (7.7)	> 0.9999
Type 3	8 (10.3)	7 (17.9)	1 (2.6)	0.0564
Type 4	39 (50.0)	17 (43.6)	22 (56.4)	0.2575
Type 5	18 (23.1)	10 (25.6)	8 (20.5)	0.5909
Type 6	5 (6.4)	3 (7.7)	2 (5.1)	> 0.9999
Type 7	2 (2.6)	0 (0)	2 (5.1)	0.4935
Exercise frequency within the past 1 year				
Often (> 6 times/week)	10 (12.8)	2 (5.1)	8 (20.5)	0.0421*
Occasionally (3–6 times/week)	23 (29.5)	11 (28.2)	12 (30.8)	0.8039
Rarely (1–2 times/week)	43 (55.1)	26 (66.7)	17 (43.6)	0.0405*
Never (0 times/week)	2 (2.6)	0 (0)	2 (5.1)	0.4935
Daily sleep duration				
< 5 h	0 (0)	0 (0)	0 (0)	–
5–6 h	14 (17.9)	9 (23.1)	5 (12.8)	0.2379
6–7 h	40 (51.3)	20 (51.3)	20 (51.3)	–
7–8 h	23 (29.5)	9 (7.7)	14 (35.9)	0.2144
> 8 h	1 (1.3)	1 (2.6)	0 (0)	> 0.9999
Dietary preferences				
Animal-based diet	19 (24.4)	11 (28.2)	8 (20.5)	0.4287
Vegetarian diet	4 (5.1)	2 (5.1)	2 (5.1)	–
Sweet diet	2 (2.6)	2 (5.1)	0 (0)	0.4935
Salty diet	10 (12.8)	5 (12.8)	5 (12.8)	–
Balanced diet	48 (61.5)	24 (61.5)	24 (61.5)	–
Mealtime regularity				
Very regular	10 (12.8)	2 (5.1)	8 (20.5)	0.0421*
Regular	53 (67.9)	26 (66.7)	27 (69.2)	0.8083

Table 1 (continued)

	Total (n = 78)	ICU staff (n = 39)	Non-medical controls (n = 39)	*P* value
Irregular	15 (19.2)	11 (28.2)	4 (10.3)	0.0443*
History of digestive diseases				
Constipation	13 (16.7)	6 (15.4)	7 (17.9)	0.7613
Frequent abdominal pain	3 (3.8)	0 (0)	3 (7.7)	0.2403
Gastroesophageal reflux	3 (3.8)	1 (2.6)	2 (5.1)	> 0.9999
Indigestion	7 (9.0)	2 (5.1)	5 (12.8)	0.4309
Food intolerance	2 (2.6)	0 (0)	2 (5.1)	0.4935
Foul-smelling flatulence or stools within the past 3 months	20 (25.6)	8 (20.5)	12 (30.8)	0.2996
Severe halitosis within the past 3 months	9 (11.5)	5 (10.3)	4 (10.3)	> 0.9999
Pollen-food allergy	5 (6.4)	3 (7.7)	2 (5.1)	> 0.9999

Values are numbers (percentages) unless stated otherwise. Abbreviations: IQR, interquartile range; n, number; BSFS, Bristol stool (form) scale. *P* values indicate differences between ICU staff and Non-ICU staff. $P < 0.05$ was considered statistically significant

To investigate whether gut microbial diversity and structure differed between ICU staff and non-medical controls, we first assessed the α-diversity within each individual. ICU staff exhibited lower microbial diversity compared to non-medical controls, which was reflected in the Chao1 index (Fig. 1A, Table S1). However, when comparing α-diversity by gender within two groups individually, no significant differences were observed (Fig. 2A).

β diversity analysis using PCA, PCoA, and NMDS demonstrated distinct segregation of bacterial community structures between ICU staff and non-medical controls (Figs. 1B–D, 2B–D). PERMANOVA and ANOSIM tests based on Bray–Curtis dissimilarity and Jaccard distance revealed significant differences in β diversity between the two groups (Fig. 1E, F). However, when comparing β-diversity by gender within each group individually, only the PERMANOVA and ANOSIM tests of Jaccard

Table 2 PERMANOVA (*adonis*) analysis of the host parameters' impact on gut microbiota using genus profiles

Confounding factor	Effect size (R^2)	*adonis* P (999 permutations)
Age	0.01199	0.502
BMI	0.00987	0.731
Gender	0.01224	0.456
Ethnic group	0.00944	0.784
Education level	0.02299	0.54
Smoking	0.01036	0.669
Working time in ICU	0.01868	0.096
Comorbidities	0.08291	0.58
BSFS	0.01217	0.466
Exercise frequency within within the past 1 months	0.0139	0.354
Daily sleep duration	0.0081	0.919
Dietary preference	0.12376	0.056
Mealtime regularity	0.02002	0.08
History of digestive diseases	0.09569	0.866
Foul-smelling flatulence or stools within the past 3 months	0.00997	0.721
Severe halitosis within the past 3 months	0.01208	0.493
Pollen-food allergy	0.01406	0.299
Grouping (ICU/non-ICU)	0.0338	**0.001*****
Grouping (doctor/nurse)	0.02257	0.643

Abbreviations: PERMANOVA, permutational multivariate analysis of variance; BMI, body mass index; ICU, intensive care unit; BSFS, Bristol stool (form) scale

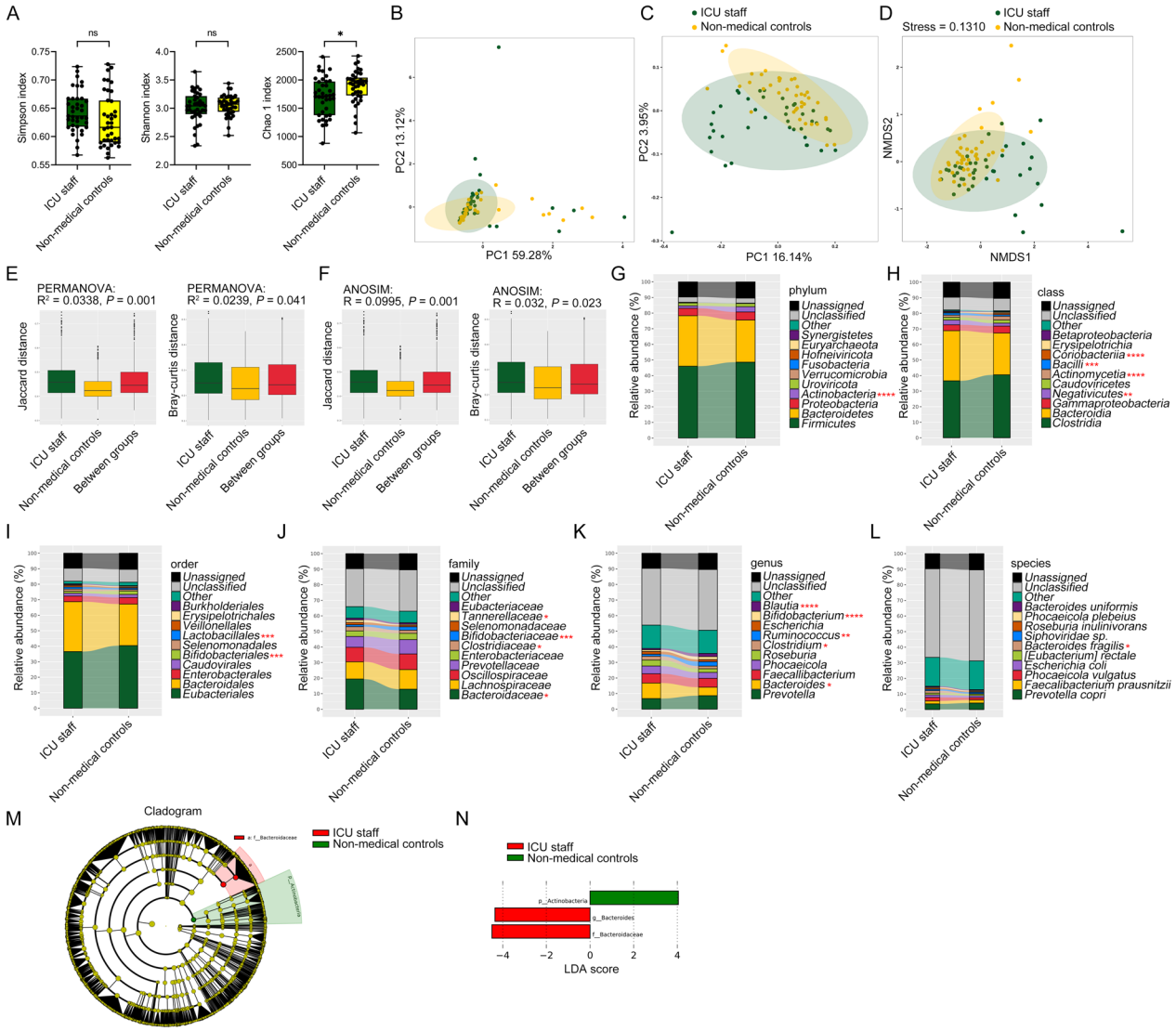

Fig. 1 Alterations in gut microbiome diversity and structure among ICU staff compared to non-medical controls. **A** Violin plots illustrate the α-diversity of gut microbiomes, as measured by Simpson, Shannon, and Chao 1 indices, for intensive care unit (ICU) staff and non-medical controls. The boxplots depict the interquartile range (IQR), with the midline indicating the median. **B** Principal component analysis (PCA), **C** Principal coordinates analysis (PCoA), and **D** non-metric multidimensional scaling (NMDS) were conducted to analyze the gut microbiome composition between the two groups. **E** Permutational multivariate analysis of variance (PERMANOVA) and **F** analysis of similarity (ANOSIM) were employed to assess statistically significant differences in β-diversity using Bray–Curtis dissimilarity and Jaccard distance metrics. The boxplots represent the IQR, with the midline indicating the median. **G**–**L** Stacked bar charts display the taxonomic composition of gut microbiomes at the phylum, class, order, family, genus, and species levels for both groups, each represented by distinct colors. **M** Cladograms generated by linear discriminant analysis effect size (LEfSe) highlight the taxonomic differences between ICU staff and non-medical controls from phylum to genus levels. **N** LEfSe analysis identified significantly differing gut microbial taxa between the two groups, with findings presented for phylum, family, and genus levels (linear discriminant analysis (LDA) score > 4.0, $P < 0.05$). $^{*}P < 0.05$; ns, not significant

distance showed significant differences among the four subgroups (Fig. 2E, F).

The abundance of gut microbiota, including taxa from the *Actinobacteria* phylum down to the *Bifidobacteriales* order, *Coriobacteriia* class, *Bifidobacteriaceae* family, and *Bifidobacterium* genus, was significantly reduced in ICU staff compared to non-medical controls. This reduction was observed exclusively in female ICU staff. Additionally, male ICU staff exhibited significantly lower levels of *Coriobacteriia* (class) and *Bifidobacteriaceae* (family). Within the *Bacteroidetes* phylum, the abundance of taxa including the *Bacteroidaceae*

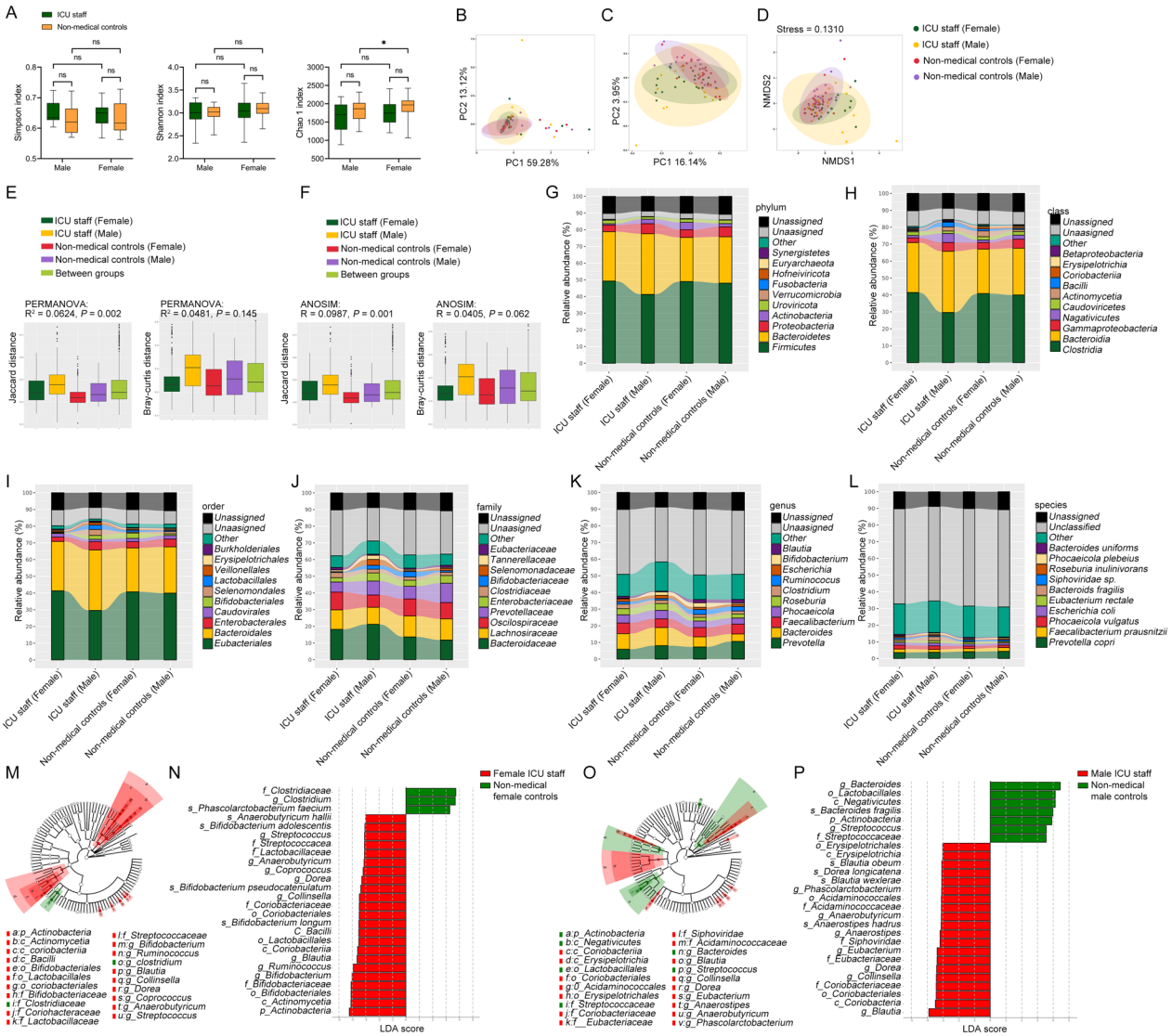

Fig. 2 Differences in the diversity and structure of gut microbiomes between ICU staff and non-medical controls within the same gender. **A** Violin plots illustrate the α-diversity of gut microbiome profiles, as measured by Simpson, Shannon, and Chao 1 indices, for intensive care unit (ICU) staff and non-medical controls. The boxplots depict the interquartile range (IQR), with the midline indicating the median. **B** Principal component analysis (PCA), **C** principal coordinates analysis (PCoA), and **D** non-metric multidimensional scaling (NMDS) were conducted to analyze the gut microbiome composition among four groups based on gender. **E** Permutational multivariate analysis of variance (PERMANOVA) and **F** analysis of similarity (ANOSIM) were employed to assess statistically significant differences in β-diversity using Bray–Curtis dissimilarity and Jaccard distance metrics. The boxplots represent the IQR, with the midline indicating the median. **G**–**L** Stacked bar charts display the taxonomic composition of gut microbiomes at the phylum, class, order, family, genus, and species levels for the four groups, each represented by distinct colors. **M**–**P** Cladograms generated using Linear Discriminant Analysis (LDA) model results highlight the bacterial hierarchy. Differences are indicated by the color of the most abundant class, with the diameter of each circle proportional to the abundance of the taxon. Each ring represents a lower taxonomic level. Linear Discriminant Analysis Effect Size (LEfSe) analysis (LDA score > 3.0, $P < 0.05$) identified genera that significantly differ among the gut microbiomes from phylum to species levels. $^{*}P < 0.05$; ns, not significant

family, *Tannerellaceae* family, *Bacteroides* genus, and *Bacteroides fragilis* species was significantly higher in ICU staff compared to non-medical controls. The significant elevation in the *Bacteroidaceae* and *Tannerellaceae* families was also observed in female ICU staff, whereas the significant increase in *Bacteroides* (genus) and *Bacteroides fragilis* (species) was exclusive to male ICU staff. Within the *Firmicutes* phylum, the abundance of taxa including the *Bacilli* family, *Negativicutes* family, *Lactobacillales* order, *Clostridiaceae* family, and *Clostridium* genus was significantly higher in ICU staff compared to non-medical controls. Male ICU staff

also exhibited lower abundances of *Siphoviridae* sp. (Figs 1G–N; 2G–P; Fig. S1; Fig. S2; Table S2).

Functional annotation analysis of gut microbiomes with GO, KEGG and EggNOG

GO analysis yielded a total of 3736 entries, including 1166 biological process entries, 174 cellular components entries, and 2396 molecular function entries (Table S3). Among the top 30 pathways, a notable decrease was observed in interspecies interaction within biological processes among ICU staff, particularly pronounced in female ICU staff. Additionally, ICU staff exhibited significant reductions in reproduction-related biological processes and toxin activity within molecular functions. In contrast, male ICU staff demonstrated a marked increase in small molecule sensor activity compared to non-medical male controls (Fig. S3A, B; Table S3).

A total of 43 KEGG pathway and 23 EggNOG orthologues groups were analyzed between the two groups. Detailed results for the top 30 KEGG pathways and all EggNOG orthologues are presented in Fig. 3A, B and Fig. S3C, D. Among these gene families, genes associated with transport and catabolism within cellular processes, as well as those implicated in endocrine and metabolic diseases, were upregulated in ICU staff, particularly in females. Additionally, genes involved in glycan biosynthesis and metabolism were significantly upregulated in ICU staff. Conversely, genes related to translation within genetic information processing were downregulated in the gut microbiomes of ICU staff, especially males, compared to controls (Fig. 3A, B, H, I; Table S4). KEGG enrichment analysis visualized the top 30 pathways using a bubble chart, displaying gene enrichment degree (x-axis), the number of enriched genes (bubble size), and *P* values (color intensity). Differentially expressed genes were predominantly found in cancer-related pathways, neuroactive ligand–receptor interactions, cytokine–cytokine receptor interactions, and other signaling pathways within the gut microbiomes of ICU staff compared to non-medical controls (Fig. 3C). Female ICU staff's gut microbiomes exhibited enriched genes related to cancer, aromatic compound degradation, ubiquitin-mediated proteolysis, and other pathways compared to non-medical females (Fig. 3J). Moreover, male ICU staff's gut microbiomes showed enriched gene expression primarily in cancer, Ras, PI3K-Akt, and other signaling pathways compared to non-medical males (Fig. 3K).

The EggNOG analysis results revealed that, irrespective of gender, the gut microbiomes of ICU staff exhibited a greater abundance of extracellular structures compared to non-medical controls (Fig. S3C, D; Table S5).

Carbohydrate active enzyme profiling of gut microbiomes

To examine differences in carbohydrate metabolism between these microbial communities, functional annotations were generated by querying the CAZy database, and hierarchical annotation was analyzed based on the distribution of six enzyme classes across the different gut microbiomes (Table S6). Overall, the enzymes annotated from the metagenomes showed a high levels of glycoside hydrolases (GHs) and glycosyltransferases (GTs) in the studied gut microbiomes. At the family level, CAZy annotations were predominantly composed of GH families (2, 3, and 13) and GT families (2 and 4). Comparative analysis revealed distinct differences between the two groups. ICU staff demonstrated substantial elevations in GHs and polysaccharide lyases (PLs), with notable enhancements in GTs and carbohydrate esterases (CEs), particularly among males. Specifically, a significant increase in carbohydrate-binding modules (CBMs) was exclusively observed in male ICU staff compared to non-medical male controls (Fig. 3D–G). Furthermore, the enzymes GT2, GH2, GT4, and GH92 were more abundant in ICU staff, especially among males. GH20 was more prevalent in ICU staff compared to non-medical controls.

(See figure on next page.)

Fig. 3 Comparison of functional annotation of gut microbiomes by KEGG and CAZy between ICU staff and non-medical controls. **A** Heatmaps depict Kyoto Encyclopedia of Genes and Genomes (KEGG) analysis from metagenomic sequencing across the general population (encompassing both genders) in intensive care unit (ICU) staff and non-medical controls, as well as within gender-stratified subpopulations (**H**). **B** Comparison of enriched KEGG orthologue group markers across 30 functional categories between the entire populations of the two groups, and between gender-matched subgroups within each cohort (**I**). **C** Dot plots illustrate KEGG pathway enrichment analysis of 30 verified genes across the general population and within gender-stratified subpopulations (**J**, **K**). In these plots, color intensity denotes the *P*-value, while dot size indicates the number of genes involved. **D** Heatmaps depict carbohydrate-degrading enzymes (CAZy) from metagenomic sequencing across the general population and within gender-stratified subpopulations (**L**). **E** CAZy comparisons were conducted between the entire populations of the two groups and among gender-specific subgroups within each cohort (**M**). **F** Heatmaps illustrate the distribution of the top 30 dominant CAZy families, categorized under various classes, across the general population and within gender-stratified subpopulations (**N**). Clustering is determined by the relative abundance of each family. **G** Functional comparisons based on CAZy classification were conducted between the entire populations of the two groups and among gender-specific subgroups within each cohort (**O**). Boxplots represent the interquartile range (IQR) between the first and third quartiles, with the midline indicating the median. $^{*}P < 0.05$, $^{**}P < 0.01$; ns, not significant

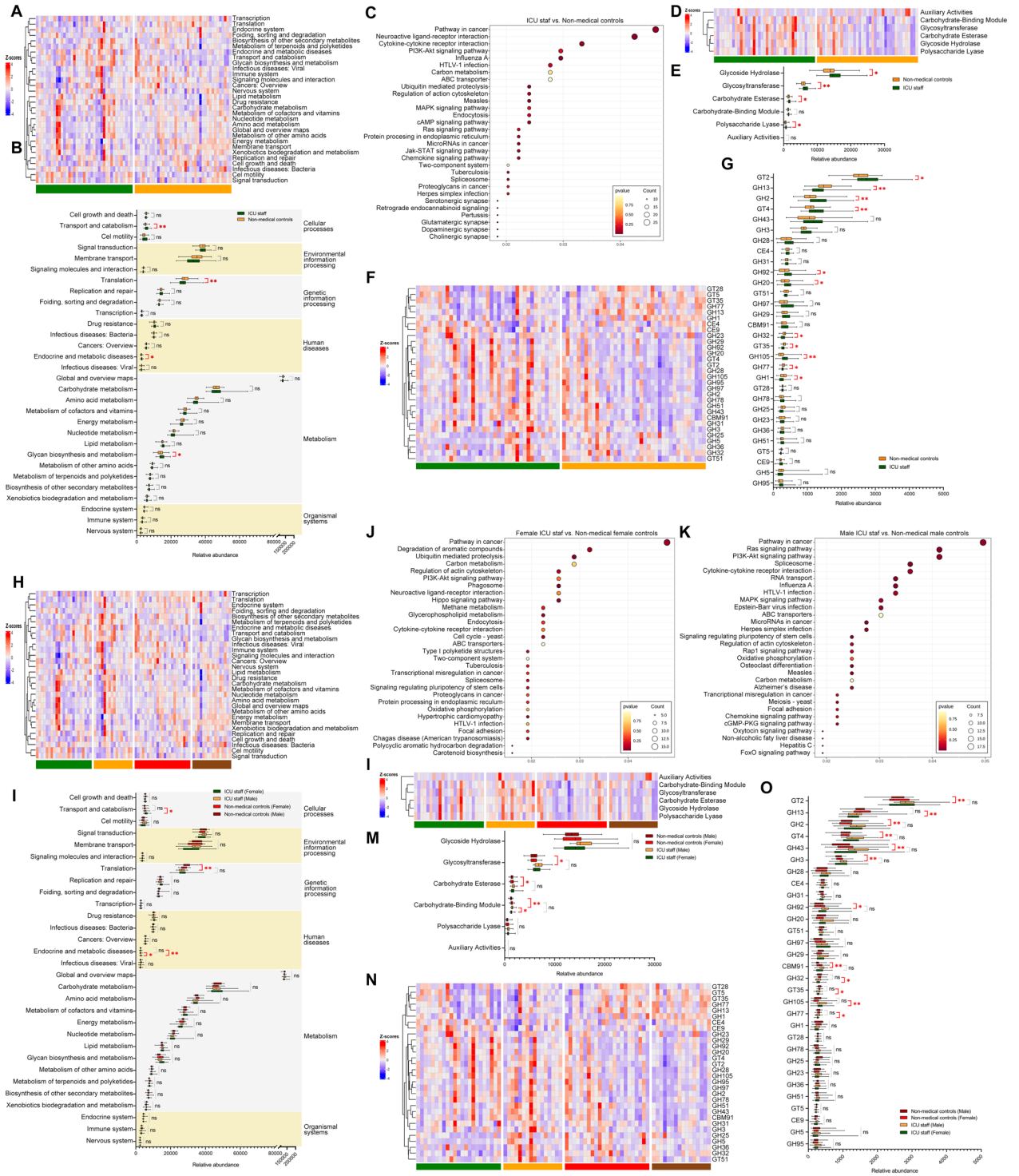

Fig. 3 (See legend on previous page.)

Conversely, enzymes such as GH13, GH32, GT35, and GH77 showed reduced abundance in ICU staff, with a particular decline observed among females. Notably, GH105 was solely more abundant in female ICU staff relative to non-medical female controls. In contrast, GH1 was less abundant in ICU staff compared to non-medical controls (Fig. 3F, G, N, O). Exclusively in male ICU staff, the enzymes GH43, GH3, and CBM91

exhibited increased abundance compared to non-medical male controls (Fig. 3L–O).

Virulence profiling of gut microbiomes

The virulence factors were categorized into the following classes: immune modulation, adherence, motility, effector delivery system, nutritional and metabolic factors, stress survival, exoenzymes, regulation, biofilm formation, post-translational modification, invasion, exotoxins, antimicrobial activity/competitive advantage, and others. ICU staff demonstrated a higher prevalence of virulence factors associated with immune modulation and antimicrobial activity/competitive advantage exclusively among females. Additionally, increased invasion capabilities were observed in ICU staff, specifically among males, compared to non-medical controls (Fig. 4A, B, D, E).

The depiction in Fig. 4C, F and Fig. S4A, B highlights the diverse functions of virulence factors from gut microbiomes among ICU staff compared to non-medical controls. The top 50 functions of VFDB emphasize this variability. Virulence factors such as Capsule, LPS, LOS, and O-antigen were observed in bacteria exhibiting enhanced glycosyltransferase activity and the presence of glycosyltransferase family 2 proteins in ICU staff, including both male and female subsets. Notably, the type III secretion apparatus (TTSS) from bacteria with increased hybrid sensor histidine kinase/response regulator activity (functioning as an effector delivery mechanism) and Capsule from bacteria with enhanced type 8 capsular polysaccharide synthesis protein (related to immune modulation) were exclusively noted in ICU staff, encompassing both genders. Moreover, the virulence factor pyoverdine from bacteria with elevated FpvR (a vital component in nutrition and metabolism), AslA (arylsulfatase-like gene) (associated with invasion mechanisms), and acriflavine resistance protein B (AcrAB; exhibiting antimicrobial activity/competitive advantage) were observed in ICU staff but were particularly prominent among male ICU staff. The virulence factor LetA/S from bacteria with increased hybrid sensor histidine kinase/response regulator (acting as a regulatory mechanism) was solely observed among male ICU staff, in contrast to non-medical male controls. TTSS-secreted effectors from bacteria with decreased glycogen hydrolase activity (acting as an effector delivery mechanism) were noted in ICU staff, with this reduction being particularly evident among female ICU staff. Decreased elongation factor Tu (integral to adherence and crucial for biofilm formation) was exclusively observed in female ICU staff. Similarly, the virulence factor BopD with decreased sugar-binding transcriptional regulator (lacI), which is also pivotal for biofilm formation, was uniquely observed among female ICU staff.

Among the top 20 drug-resistant bacterial species reported in the 'Antimicrobial Resistance Profile of Clinical Isolates in Hospitals Across China: Report from the CHINET Antimicrobial Resistance Surveillance Program, 2023' [19], 10 species were found to secrete virulence factors (Fig. 5). The abundance of virulence factors in ICU staff was significantly elevated compared to non-medical controls. Specifically, these included LPS, Phospholipase C, HemO cluster, and Ata from *Acinetobacter baumannii*; AslA from *Escherichia coli*; HxuABC from *Haemophilus influenzae*; AcrAB from *Klebsiella pneumoniae*; LPS, Pyoverdine, and Flagella from *Pseudomonas aeruginosa*; and CbpA/PspC and PsaA from *Streptococcus pneumoniae*. Notably, the virulence factors unique to *Acinetobacter baumannii* were exclusively detected in ICU staff and absent from non-medical controls. Conversely, the levels of T2SS from *Acinetobacter baumannii,* AS, Cytolysin, and Ebp pili from *Enterococcus faecalis*; Scm, Acm, and EcbA from *Enterococcus faecium*; Paa, BFP, and Per from *Escherichia coli*; HSI-I from *Pseudomonas aeruginosa*; Clumping factor and CNA from *Staphylococcus aureus;* β-hemolysin/cytolysin, PI-1, and PI-2a from *Streptococcus agalactiae*; and RlrA islet and PI-2 from *Streptococcus pneumoniae* were notably lower in ICU staff compared to non-medical controls (Fig. 5).

Resistance gene annotation analysis of gut microbiomes

Metagenomics and computational methods serve as potent molecular tools for investigating microbial communities, ARGs, and their interrelations across diverse samples, eliminating the need for isolating pure cultures [20]. Through high-throughput sequencing-based metagenomics analyses using a CARD database, 263 CARD AROs belonging to 31 drug classes were identified. The majority of the top 30 AROs exhibited resistance to a single drug class, with the exception of *adeF*, *qacG*, *ErmB*, *Erm(35)*, *ErmF*, and *tet(X)*, which conferred resistance to disinfecting agents and antiseptics, fluoroquinolones, glycylcyclines, lincosamides, macrolides, streptogramins A and B, and tetracycline (Table S7). Overall, there was no significant disparity in the abundance of AROs between the two groups (Fig. 6A). Notably, the abundance of ARO *adeF*, an efflux pump conferring resistance to fluoroquinolones and tetracyclines, was significantly increased in ICU staff compared to non-medical controls. Conversely, the overall abundance of specific AROs, including *Tet(t)* (resistant to tetracycline via antibiotic target protection), *Tet(40)* (resistant to tetracycline through efflux pump mechanisms), *dfrF* (resistant to diaminopyrimidines by antibiotic target replacement), and *vanU_in_vanG_cl* (resistant to glycopeptides due to antibiotic target alteration), was decreased in ICU staff,

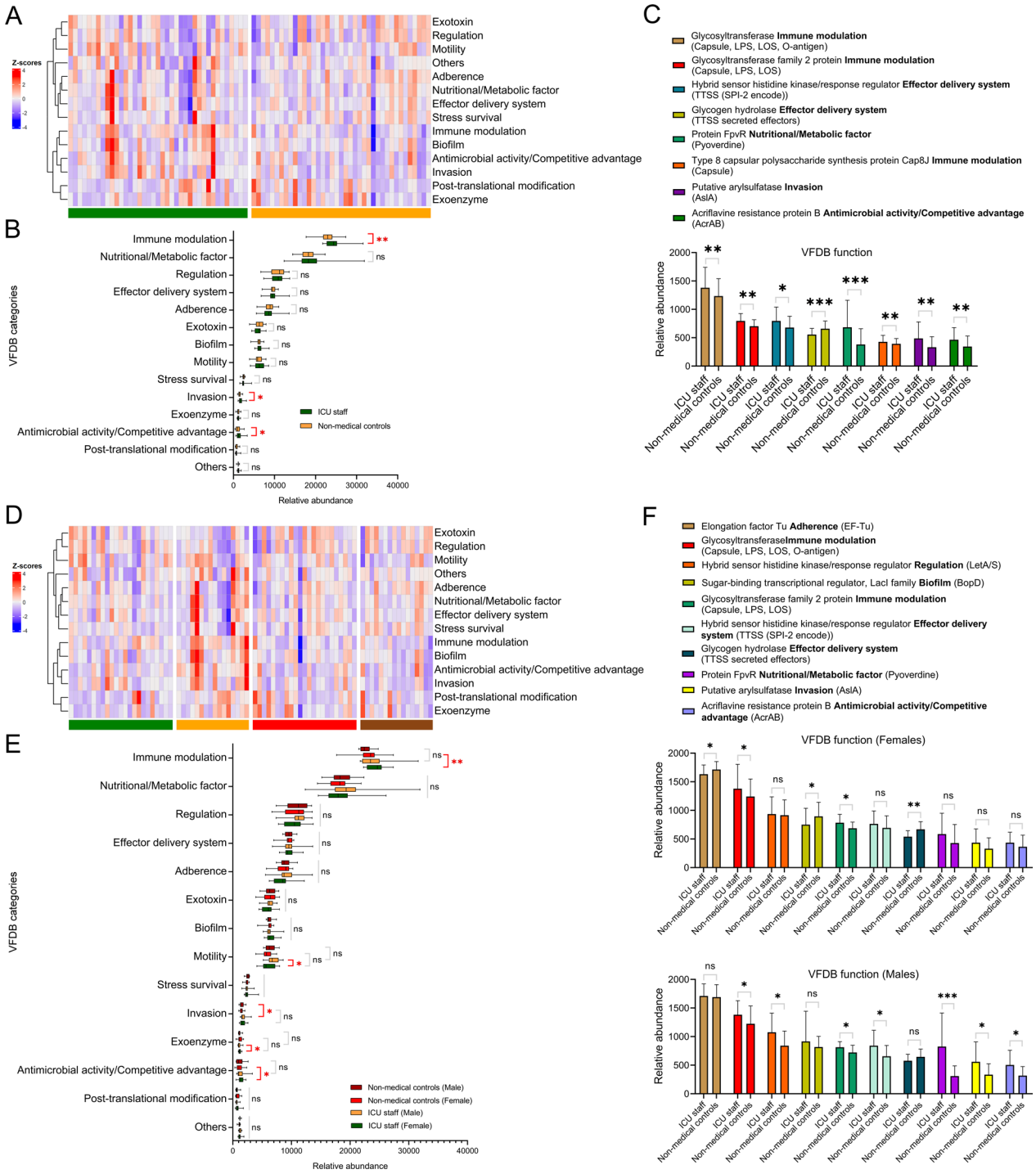

Fig. 4 Comparison of virulence factors from gut microbiomes between ICU staff and non-medical controls. **A** Heatmaps depict virulence categories aligned from the Virulence Factor Database (VFDB) within gut microbiomes across the entire population (both genders included) of intensive care unit (ICU) staff and non-medical controls, as well as comparing gender-specific subgroups within each cohort (**D**). **B** Comparison of virulence categories between the entire populations of both groups, and within gender-specific subsets within each cohort (**E**). **C** Heatmaps and comparative analysis illustrate key functions of VFDB across the entire populations of both groups, as well as within gender-specific subgroups within each cohort (**F**). Boxplots represent the interquartile range (IQR) between the first and third quartiles, with the midline indicating the median. $^{*}P<0.05$, $^{**}P<0.01$, $^{***}P<0.001$; ns, not significant

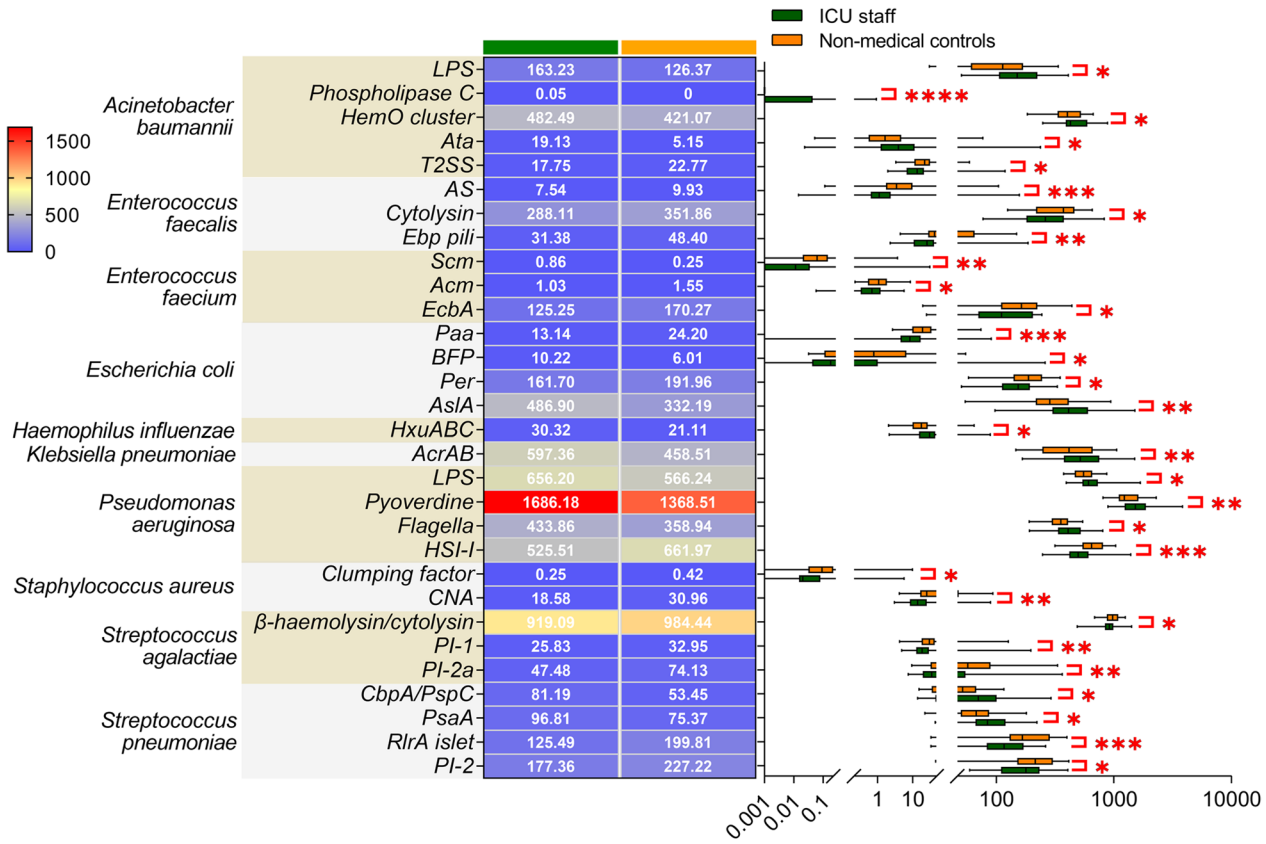

Fig. 5 Differences in virulence factors from nine drug-resistant bacterial species in the gut microbiomes among the Top 20 most common antibiotic-resistant bacteria in China between ICU staff and non-medical controls. Boxplots represent the interquartile range (IQR) between the first and third quartiles, with the midline indicating the median. $^{*}P<0.05$, $^{**}P<0.01$, $^{***}P<0.001$, $^{****}P<0.0001$

particularly among males, compared to non-medical controls. Additionally, the abundance of ARO *dfrF* was also significantly decreased in female ICU staff compared to non-medical female controls. Furthermore, a notable decline in the presence of AROs *tet(O)* (resistant to tetracycline via antibiotic target protection) and *nimJ* (resistant to nitroimidazoles via antibiotic inactivation) was exclusively observed among male ICU staff, in contrast to non-medical male controls (Fig. 6B, C).

The bacteria *Parabacteroides distasonis* and *Bacteroides fragilis*, harboring ARGs, exhibited significantly elevated levels in ICU staff, particularly among males, compared to non-medical controls. Conversely, other

(See figure on next page.)

Fig. 6 Variations in the composition and abundance of AROs detected by CARD between ICU staff and non-medical controls. **A** Comparison of the total abundance of antibiotic resistance ontologies (AROs) between intensive care unit (ICU) staff and non-medical controls. **B** Comparison of the abundance of the top 30 abundant AROs across the entire population (encompassing both genders) of the two groups, as well as between gender-specific subgroups within each cohort (**C**). **D** Comparison of the top 30 abundant bacteria harboring AROs across the entire population of the two groups, as well as within gender-specific subgroups within each cohort (**E**). **F** Heatmaps depict the six drug-resistant bacterial species among the top 20 most common antibiotic-resistant bacteria in China across the total population (inclusive of both genders) of the two groups, further differentiated between gender-specific subgroups within each cohort (**H**). **G** Comparison of the abundance of six drug-resistant bacterial species across the entire populations of the two groups, as well as among gender-specific subgroups within each cohort (**I**). **J**–**O** Circle maps illustrate the attribution analysis of AROs and bacterial species among various groups: ICU staff (**J**), non-medical controls (**K**), female ICU staff (**L**), male ICU staff (**M**), non-medical female controls (**N**), and non-medical male controls (**O**). The inner circle depicts the distribution of AROs within each species, while the outer circle outlines the species distribution of all sample genes within the respective group. Boxplots represent the interquartile range (IQR) between the first and third quartiles, with the midline indicating the median. $^{*}P<0.05$, $^{**}P<0.01$, $^{***}P<0.001$, $^{****}P<0.0001$; ns, not significant

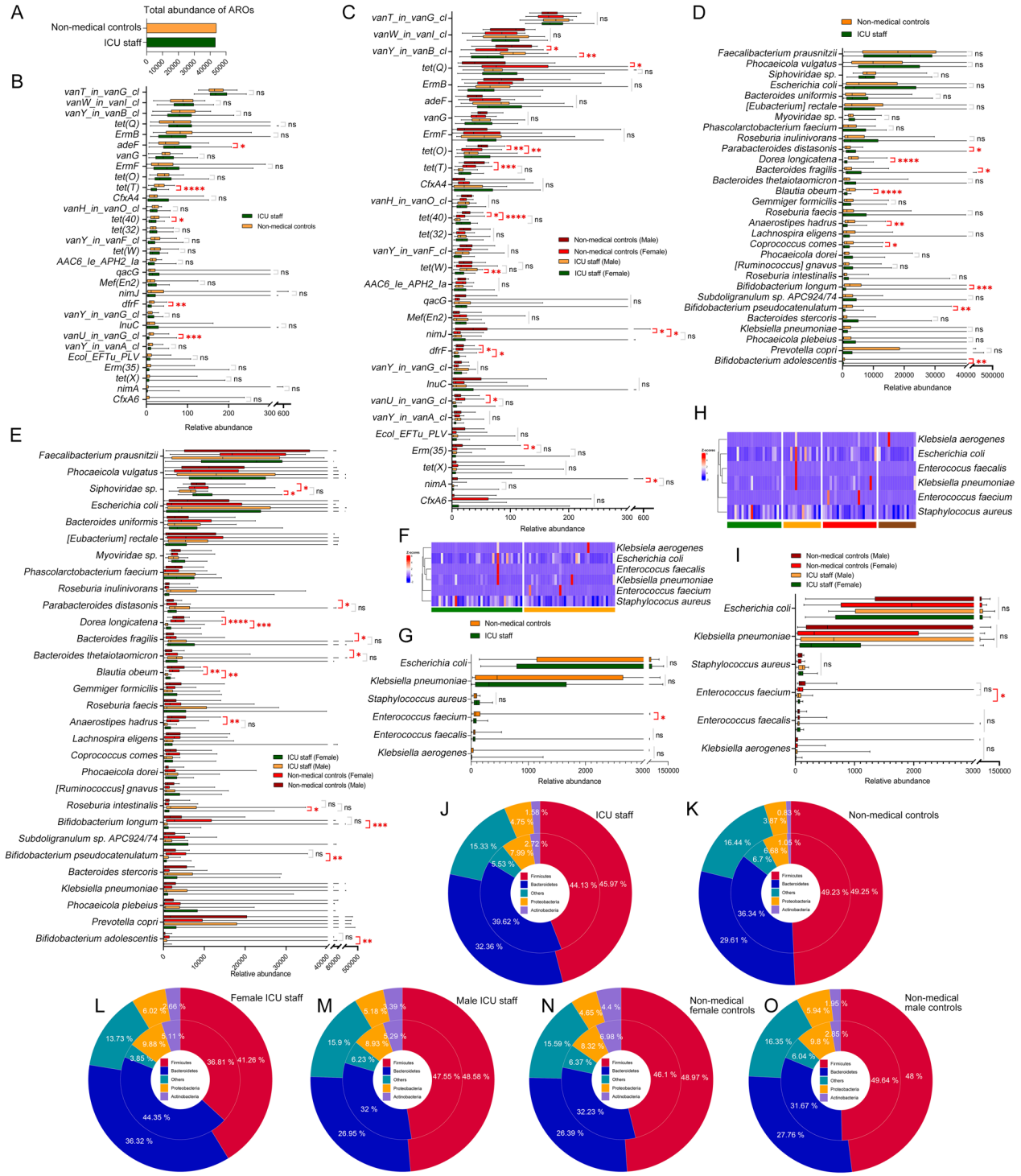

Fig. 6 (See legend on previous page.)

bacteria carrying ARGs, namely *Dorea longicaten*a and *Blautia obeum*, displayed notably decreased abundance in ICU staff, including both male and female subsets. Specifically, *Siphoviridae sp.* showed a significant reduction exclusively among male ICU staff relative to non-medical male controls. *Anaerostipes hadrus* was also significantly decreased in ICU staff, with a particular emphasis on male ICU staff, relative to non-medical

controls. *Coprococcus comes* was less abundant in ICU staff compared to non-medical controls. Furthermore, *Bifidobacterium longum*, *Bifidobacterium pseudocatenulatum*, and *Bifidobacterium adolescentis* exhibited significantly reduced abundance in ICU staff, particularly among females, when compared to non-medical controls (Fig. 6D, E, Table S7).

For specific antibiotics, overall, no discernible difference was observed in the relative abundance of AROs between the two groups. The relatively low abundance of AROs conferring resistance to oxazolidinone in ICU staff, particularly among females, compared to non-medical controls, suggests that any increase in their prevalence is of minimal significance (Fig. S5A; Table S8). Nevertheless, male ICU staff exhibited a lower abundance of AROs conferring resistance to both streptogramin A and streptogramin B compared to non-medical male controls (Fig. S5B).

Among the top 20 drug-resistant bacterial species reported in the 'Antimicrobial Resistance Profile of Clinical Isolates in Hospitals Across China: Report from the CHINET Antimicrobial Resistance Surveillance Program, 2023' [19], only six drug-resistant bacterial species were detected in our analyzed samples: *Escherichia coli*, *Klebsiella pneumoniae*, *Staphylococcus aureus*, *Enterococcus faecium*, *Enterococcus faecalis*, and *Klebsiella aerogenes* (Fig. 6F, G; Table S9). Remarkably, ICU staff, particularly female staff, exhibited lower levels of *Enterococcus faecium* compared to non-medical controls. However, no significant differences were observed between the two groups for the other five drug-resistant bacterial species across both genders (Fig. 6H, I).

Correlation between AROs and microbial communities

The occurrence of AROs generally correlates with the structure and composition of bacterial communities. Therefore, this study also examined the correlation between bacterial community structure and ARO profiles. *Firmicutes* and *Bacteroidetes* were the two predominant phyla in antibiotic-resistant bacteria among samples collected from ICU staff and non-medical controls, irrespective of gender (Fig. 6J–P).

Discussion

Research utilizing 16S rRNA amplicon sequencing has demonstrated differences in the gut microbiome between ICU staff and non-medical controls [6]. Our study reveals distinct gut microbiome diversity, composition, phenotypes, and functions in ICU staff through metagenomic sequencing. Gender-based discrepancies are also observed.

Microbial communities are essential for sustaining healthy ecosystems. In our study, ICU staff exhibited reduced gut microbiome diversity, with lower levels of *Actinobacteria* and higher levels of *Bacteroides*/*Bacteroidaceae*. Both genders showed decreased gut microbiota abundance. Actinobacteria, a key phylum, produce diverse secondary metabolites that maintain gut homeostasis, regulate immunity, and generate antibiotics, antifungals, and anticancer compounds [21–23]. Specifically, *Bifidobacteria*, a genus within *Actinobacteria*, contribute to gut barrier maintenance through the production of SCFAs like acetate and butyrate [21]. Butyrate positively correlates with increased expression of the MUC2 gene, which encodes a mucin glycoprotein essential for forming the mucous layer and maintaining the intestinal barrier [24]. Among alcohol-dependent individuals, increased intestinal permeability is associated with reduced *Bifidobacteria* levels [25]. Lower *Bifidobacteria* levels could increase gut permeability, facilitating LPS translocation into the bloodstream [26]. *Actinobacteria* aid in carbohydrate and fatty acid metabolism, immunoinflammatory regulation, and the biodegradation of resistant starch [27–29]. Specifically, *Bifidobacteria* utilize GHs to hydrolyze glycosidic bonds, degrading plant-derived carbohydrates such as starch and polysaccharides [30–32]. They also convert linoleic acid into conjugated linoleic acids, which offer health benefits including anti-cancer, anti-atherosclerosis, anti-diabetes, and anti-obesity properties, as well as enhanced immunity [33, 34]. *Actinobacteria*, particularly *Bifidobacteria*, modulate immune responses by inducing regulatory T-cells [35, 36], making them of significant interest for probiotic applications [21]. Conversely, *Bacteroides fragilis*, a prominent gut bacterium, exhibits pro-oncogenic properties, competes for nutrients, contributes to autoimmune disorders, and acts as a multi-site pathogen [37–41]. Disturbances in the gut microbiome may pose risks to ICU staff, evident from increased endocrine/metabolic risks, especially in females, and activation of cancer-related pathways as indicated by KEGG analysis.

ICU staff exhibited a higher prevalence of virulence factors linked to immune modulation (females), invasion (males), and antimicrobial activity (females), as revealed by VFDB analysis. Our study reveals that ICU staff with high GT activity may exhibit enhanced immune modulation related to virulence, primarily through synthesizing bacterial components like Capsule, LPS, LOS, and O-antigen. Elevated levels of hybrid sensor histidine kinase/response regulators in ICU staff could enhance effector delivery via TTSS, crucial for virulence in Gram-negative bacteria [42]. Pyoverdine from the gut microbiomes of ICU staff may translocate into the host, bind to iron, impair mitochondrial function, trigger mitophagy, and cause mitochondrial damage [43]. Elevated levels of

AslA from *Escherichia coli* in ICU staff may enhance the pathogen's ability to cross the blood–brain barrier, potentially leading to meningitis [44]. Increased expression of the efflux pump AcrAB from *Klebsiella pneumoniae* in ICU staff may contribute to antimicrobial resistance and pathogenesis [45, 46].

Variations in the diversity and composition of gut microbiomes among ICU staff may result in notable metabolic differences compared to non-medical controls. Specifically, ICU staff exhibited a substantial increase in glycan biosynthesis and metabolism, as evidenced by KEGG analysis. This was paralleled by a significant elevation in carbohydrate-active enzymes (including GHs, GTs, CEs, and PLs) in ICU staff, as annotated by CAZy. Notably, a particularly pronounced increase was observed in male ICU staff.

MDRO-infected individuals and carriers may pose a significant risk of spreading infection in ICUs, where ARGs may be promiscuously spread via various mechanisms. For example, carbapenem-resistant *pOXA-48* plasmids could transfer both between and within patients, primarily mediated by ST11 *Klebsiella pneumoniae*. This strain could colonize patients and transfer the plasmid to other *Enterobacteriaceae* species, including *Escherichia coli*, *Citrobacter freundii*, and *Enterobacter cloacae* [7]. Super-spreaders of carbapenem-resistant *Enterobacteriaceae* exist, with frequent *pOXA-48* transmission observed in specific wards and single rooms within wards [7]. Despite differences in gut microbiome diversity, our study found no significant overall difference in ARG abundance between ICU staff and non-medical controls. However, male ICU staff exhibited higher levels of *adeF* but lower levels of *tet(t)*, *tet(40)*, *dfrF*, and *vanU_in_vanG_cl*. No significant difference in antibiotic resistance based on gut microbiome resistance genes was observed between groups. Nevertheless, ICU staff showed significantly increased abundances of *Bacteroides fragilis* carrying ARGs. *Bacteroides* could cause intra-abdominal infections and bacteremia due to compromised intestinal walls [37, 47, 48]. Additional potential infections caused by *Bacteroides* include skin, respiratory, and cerebral abscesses [37, 48, 49].

Intestinal dysbiosis could influence the development of enterogenic sepsis and lung infections [50–52]. Among the top 20 antibiotic-resistant bacteria identified in the CARD 2023 [19], six were detected in both ICU staff and non-medical controls. Notably, *Enterococcus faecium* levels were reduced in ICU staff, particularly among females. Among the 20 most prevalent drug-resistant infections, there was a significant increase in virulence factors originating from various pathogens in ICU staff. These include LPS, Phospholipase C, the HemO cluster, and Ata from *Acinetobacter baumannii*; AslA from *Escherichia coli*; HxuABC from *Haemophilus influenzae*; AcrAB from *Klebsiella pneumoniae*; LPS, Pyoverdine, and Flagella from *Pseudomonas aeruginosa*; and CbpA/PspC and PsaA from *Streptococcus pneumoniae*. Surprisingly, virulence factors derived from *Acinetobacter baumannii* were exclusively found in ICU staff. Among these virulence factors, Phospholipase C facilitates bacterial invasion, while Ata plays a key role in adhesion to host matrices and membranes (Table S10). Nevertheless, the current study employing metagenomics and strain-level identification cannot definitively ascertain the transmission dynamics of ARGs. It remains unclear whether the transfer of ARGs occurs between patients, within individual patients, or between patients and ICU staff.

Limitations

This study has several limitations. First, the lack of a longitudinal design prevents establishing temporal variations in gut microbiomes between ICU staff and non-medical controls. Second, while distinct taxonomic and functional features were observed, metagenomic functional analysis, though superior to 16S rRNA amplicon sequencing, could not elucidate causal relationships or assess long-term health implications. Third, the limited sample size, especially when stratified by gender, may weaken statistical power and increase the risk of Type II errors. Additionally, the study included only healthy ICU staff from a single center and 39 healthy non-medical individuals, potentially introducing selection bias. Another limitation is the exclusive focus on fecal samples, neglecting other microbiota sources like oral, skin, or urinary tract samples. The exclusion of medical workers from general wards also limits the comparison of gut microbiota composition and function. Lastly, the absence of environmental samples related to the ICU environment adds another limitation.

Conclusions

This study reveals that ICU staff exhibit reduced gut microbiome diversity, elevated levels of virulence factors (especially from drug-resistant bacteria), increased carbohydrate-active enzymes, and higher risks of endocrine/metabolic diseases and cancer, with notable gender-specific variations. Notably, no significant difference in ARG abundance was observed between ICU staff and non-medical controls. Monitoring and enhancing the gut microbiomes of ICU staff is imperative. Healthcare professionals, particularly those in ICUs, should urgently prioritize their personal health.

Abbreviations

ICU	Intensive care unit
MDROs	Multidrug-resistant organisms
ARGs	Antibiotic resistance genes

GO	Gene ontology
KEGG	Kyoto Encyclopedia of Genes and Genomes
eggNOG	Evolutionary genealogy of genes: Non-supervised Orthologous Groups
CAZy	Carbohydrate-active enZymes
VFDB	Virulence factor database
CARD	Comprehensive antibiotic resistance database
BMI	Body mass index
BSFS	Bristol stool form scale
PCA	Principal component analysis
PCoA	Principal co-ordinates analysis
NMDS	Non-metric multidimensional scaling
PERMANOVA	Permutational multivariate analysis of variance
ANOSIM	Analysis of similarity
GHs	Glycoside hydrolases
GTs	Glycosyl transferases
CBMs	Carbohydrate-binding modules
CEs	Carbohydrate esterases

Supplementary Information

The online version contains supplementary material available at https://doi.org/10.1186/s13054-025-05379-7.

Additional file 1: Table S6

Additional file 2: Table S7

Additional file 3: Table S8

Additional file 4: Table S9

Additional file 5: Supplemental Figures

Additional file 6: Table S1

Additional file 7: Table S10

Additional file 8: Table S2

Additional file 9: Table S3

Additional file 10: Table S4

Additional file 11: Table S5

Acknowledgements
We thank all the ICU staff and non-medical subjects who participated in this trial.

Author contributions
Jiancheng Zhang, Xing Zhao, You Shang and Yongling Lv conceived the study, designed experiments and analyzed the metagenomic sequencing data. Bing Xie, Chenyang Dong, Xin Zhao, Lianlian Qu, Hong Liu, Jiaxin Xu, Zhizhong Yu conducted research. Jiancheng Zhang interpreted the results. Jiancheng Zhang wrote the manuscript, which was further refined by Yongling Lv and Bing Xie. Hexiao Shen supervised the overall study.

Funding
The study was funded by the National Natural Science Foundation of China (Grant No. 82472223 [to JCZ]; Grant No. 82402568 [to BX]).

Availability of data and materials
All metagenomic sequencing raw data was uploaded to NCBI BioProject and is publicly available (http://www.ncbi.nlm.nih.gov/bioproject/1208576). The clinical data that support the findings of this study are available from the corresponding author, Jiancheng Zhang, upon reasonable request.

Declarations

Ethics approval and consent to participate
This study protocol was approved by the Ethics Committee of Union Hospital, Tongji Medical College, Huazhong University of Science and Technology (Approval No. 0468). This study was registered with the ClinicalTrials: NCT06524765, date of registration: 07/11/2024. Written informed consent was obtained from each participant.

Consent for publication
All listed authors consent to the submission, and all data are used with the consent of the person generating the data.

Competing interests
The authors declare no competing interests.

Author details
[1]Department of Critical Care Medicine, Union Hospital, Tongji Medical College, Huazhong University of Science and Technology, Wuhan 430022, China. [2]Key Laboratory of Anesthesiology and Resuscitation (Huazhong University of Science and Technology), Ministry of Education, Wuhan 430030, China. [3]Department of Nursing, Union Hospital, Tongji Medical College, Huazhong University of Science and Technology, Wuhan 430022, China. [4]School of Life Science, Hubei University, Wuhan 430000, China.

Received: 23 January 2025 Accepted: 19 March 2025
Published online: 31 March 2025

References

1. Corriero A, Gadaleta RM, Puntillo F, Inchingolo F, Moschetta A, Brienza N. The central role of the gut in intensive care. Crit Care. 2022;26(1):379. https://doi.org/10.1186/s13054-022-04259-8.
2. Dickson RP. The microbiome and critical illness. Lancet Respir Med. 2016;4(1):59–72. https://doi.org/10.1016/S2213-2600(15)00427-0.
3. Lankelma JM, Cranendonk DR, Belzer C, de Vos AF, de Vos WM, van der Poll T, Wiersinga WJ. Antibiotic-induced gut microbiota disruption during human endotoxemia: a randomised controlled study. Gut. 2017;66(9):1623–30. https://doi.org/10.1136/gutjnl-2016-312132.
4. Schlechte J, Zucoloto AZ, Yu IL, Doig CJ, Dunbar MJ, Mccoy KD, Mcdonald B. Dysbiosis of a microbiota-immune metasystem in critical illness is associated with nosocomial infections. Nat Med. 2023;29(4):1017–27. https://doi.org/10.1038/s41591-023-02243-5.
5. Cho NA, Strayer K, Dobson B, Mcdonald B. Pathogenesis and therapeutic opportunities of gut microbiome dysbiosis in critical illness. Gut Microbes. 2024;16(1):2351478. https://doi.org/10.1080/19490976.2024.2351478.
6. Zheng N, Li SH, Dong B, Sun W, Li HR, Zhang YL, Li P, Fang ZW, Chen CM, Han XY, et al. Comparison of the gut microbiota of short-term and long-term medical workers and non-medical controls: a cross-sectional analysis. Clin Microbiol Infect. 2021;27(9):1285–92. https://doi.org/10.1016/j.cmi.2020.10.033.
7. Leon-Sampedro R, Delafuente J, Diaz-Agero C, Crellen T, Musicha P, Rodriguez-Beltran J, de la Vega C, Hernandez-Garcia M, Lopez-Fresnena N, Ruiz-Garbajosa P, et al. Pervasive transmission of a carbapenem resistance plasmid in the gut microbiota of hospitalized patients. Nat Microbiol. 2021;6(5):606–16. https://doi.org/10.1038/s41564-021-00879-y.
8. Kumar H, Park W, Lim D, Srikanth K, Kim JM, Jia XZ, Han JL, Hanotte O, Park JE, Oyola SO. Whole metagenome sequencing of cecum microbiomes in ethiopian indigenous chickens from two different altitudes reveals antibiotic resistance genes. Genomics. 2020;112(2):1988–99. https://doi.org/10.1016/j.ygeno.2019.11.011.
9. Ma ZS, Li W. How and why men and women differ in their microbiomes: medical ecology and network analyses of the microgenderome. Adv Sci (Weinh). 2019;6(23):1902054. https://doi.org/10.1002/advs.201902054.
10. Zhang X, Zhong H, Li Y, Shi Z, Ren H, Zhang Z, Zhou X, Tang S, Han X, Lin Y, et al. Sex- and age-related trajectories of the adult human gut microbiota shared across populations of different ethnicities. Nat Aging. 2021;1(1):87–100. https://doi.org/10.1038/s43587-020-00014-2.
11. Buchfink B, Xie C, Huson DH. Fast and sensitive protein alignment using diamond. Nat Methods. 2015;12(1):59–60. https://doi.org/10.1038/nmeth.3176.
12. Bagci C, Patz S, Huson DH. Diamond+megan: fast and easy taxonomic and functional analysis of short and long microbiome sequences. Curr Protoc. 2021;1(3): e59. https://doi.org/10.1002/cpz1.59.

13. Aramaki T, Blanc-Mathieu R, Endo H, Ohkubo K, Kanehisa M, Goto S, Ogata H. Kofamkoala: kegg ortholog assignment based on profile hmm and adaptive score threshold. Bioinformatics. 2020;36(7):2251–2. https://doi.org/10.1093/bioinformatics/btz859.
14. Paulson JN, Stine OC, Bravo HC, Pop M. Differential abundance analysis for microbial marker-gene surveys. Nat Methods. 2013;10(12):1200–2. https://doi.org/10.1038/nmeth.2658.
15. Cantalapiedra CP, Hernandez-Plaza A, Letunic I, Bork P, Huerta-Cepas J. Eggnog-mapper v2: functional annotation, orthology assignments, and domain prediction at the metagenomic scale. Mol Biol Evol. 2021;38(12):5825–9. https://doi.org/10.1093/molbev/msab293.
16. Alcock BP, Huynh W, Chalil R, Smith KW, Raphenya AR, Wlodarski MA, Edalatmand A, Petkau A, Syed SA, Tsang KK, et al. Card 2023: expanded curation, support for machine learning, and resistome prediction at the comprehensive antibiotic resistance database. Nucleic Acids Res. 2023;51(D1):D690–9. https://doi.org/10.1093/nar/gkac920.
17. Zhang H, Yohe T, Huang L, Entwistle S, Wu P, Yang Z, Busk PK, Xu Y, Yin Y. Dbcan2: a meta server for automated carbohydrate-active enzyme annotation. Nucleic Acids Res. 2018;46(W1):W95–101. https://doi.org/10.1093/nar/gky418.
18. Liu B, Zheng D, Jin Q, Chen L, Yang J. Vfdb 2019: a comparative pathogenomic platform with an interactive web interface. Nucleic Acids Res. 2019;47(D1):D687–92. https://doi.org/10.1093/nar/gky1080.
19. Yan G, Fupin H, Demei Z, Lin L, Zhuo Z, Jianlong L, Min F, Yinghui G, Wenchao Z, Zengguo W, et al. Antimicrobial resistance profile of clinical isolates in hospitals across china: report from the chinet antimicrobial resistance surveillance program, 2023. Chin J Infect Chemother. 2024;24(06):627–37. https://doi.org/10.16718/j.1009-7708.2024.06.001.
20. Laudadio I, Fulci V, Stronati L, Carissimi C. Next-generation metagenomics: methodological challenges and opportunities. OMICS. 2019;23(7):327–33. https://doi.org/10.1089/omi.2019.0073.
21. Binda C, Lopetuso LR, Rizzatti G, Gibiino G, Cennamo V, Gasbarrini A. Actinobacteria: a relevant minority for the maintenance of gut homeostasis. Dig Liver Dis. 2018;50(5):421–8. https://doi.org/10.1016/j.dld.2018.02.012.
22. Alwali AY, Parkinson EI. Small molecule inducers of actinobacteria natural product biosynthesis. J Ind Microbiol Biotechnol. 2023;50(1):kuad019. https://doi.org/10.1093/jimb/kuad019.
23. Barka EA, Vatsa P, Sanchez L, Gaveau-Vaillant N, Jacquard C, Meier-Kolthoff JP, Klenk HP, Clement C, Ouhdouch Y, van Wezel GP. Taxonomy, physiology, and natural products of actinobacteria. Microbiol Mol Biol Rev. 2016;80(1):1–43. https://doi.org/10.1128/MMBR.00019-15.
24. Willemsen LE, Koetsier MA, van Deventer SJ, van Tol EA. Short chain fatty acids stimulate epithelial mucin 2 expression through differential effects on prostaglandin e(1) and e(2) production by intestinal myofibroblasts. Gut. 2003;52(10):1442–7. https://doi.org/10.1136/gut.52.10.1442.
25. Leclercq S, Matamoros S, Cani PD, Neyrinck AM, Jamar F, Starkel P, Windey K, Tremaroli V, Backhed F, Verbeke K, et al. Intestinal permeability, gut-bacterial dysbiosis, and behavioral markers of alcohol-dependence severity. Proc Natl Acad Sci USA. 2014;111(42):E4485–93. https://doi.org/10.1073/pnas.1415174111.
26. Duca FA, Sakar Y, Covasa M. The modulatory role of high fat feeding on gastrointestinal signals in obesity. J Nutr Biochem. 2013;24(10):1663–77. https://doi.org/10.1016/j.jnutbio.2013.05.005.
27. Macfarlane GT, Englyst HN. Starch utilization by the human large intestinal microflora. J Appl Bacteriol. 1986;60(3):195–201. https://doi.org/10.1111/j.1365-2672.1986.tb01073.x.
28. Ryan SM, Fitzgerald GF, van Sinderen D. Screening for and identification of starch-, amylopectin-, and pullulan-degrading activities in bifidobacterial strains. Appl Environ Microbiol. 2006;72(8):5289–96. https://doi.org/10.1128/AEM.00257-06.
29. Salyers AA, West SE, Vercellotti JR, Wilkins TD. Fermentation of mucins and plant polysaccharides by anaerobic bacteria from the human colon. Appl Environ Microbiol. 1977;34(5):529–33. https://doi.org/10.1128/aem.34.5.529-533.1977.
30. Pokusaeva K, Fitzgerald GF, van Sinderen D. Carbohydrate metabolism in bifidobacteria. Genes Nutr. 2011;6(3):285–306. https://doi.org/10.1007/s12263-010-0206-6.
31. El KA, Armougom F, Gordon JI, Raoult D, Henrissat B. The abundance and variety of carbohydrate-active enzymes in the human gut microbiota. Nat Rev Microbiol. 2013;11(7):497–504. https://doi.org/10.1038/nrmicro3050.
32. Milani C, Lugli GA, Duranti S, Turroni F, Mancabelli L, Ferrario C, Mangifesta M, Hevia A, Viappiani A, Scholz M, et al. Bifidobacteria exhibit social behavior through carbohydrate resource sharing in the gut. Sci Rep. 2015;5:15782. https://doi.org/10.1038/srep15782.
33. Raimondi S, Amaretti A, Leonardi A, Quartieri A, Gozzoli C, Rossi M. Conjugated linoleic acid production by bifidobacteria: screening, kinetic, and composition. Biomed Res Int. 2016;2016:8654317. https://doi.org/10.1155/2016/8654317.
34. Kim JH, Kim Y, Kim YJ, Park Y. Conjugated linoleic acid: potential health benefits as a functional food ingredient. Annu Rev Food Sci Technol. 2016;7:221–44. https://doi.org/10.1146/annurev-food-041715-033028.
35. O'Mahony C, Scully P, O'Mahony D, Murphy S, O'Brien F, Lyons A, Sherlock G, Macsharry J, Kiely B, Shanahan F, et al. Commensal-induced regulatory t cells mediate protection against pathogen-stimulated nf-kappab activation. Plos Pathog. 2008;4(8):e1000112. https://doi.org/10.1371/journal.ppat.1000112.
36. Lyons A, O'Mahony D, O'Brien F, Macsharry J, Sheil B, Ceddia M, Russell WM, Forsythe P, Bienenstock J, Kiely B, et al. Bacterial strain-specific induction of foxp3+ t regulatory cells is protective in murine allergy models. Clin Exp Allergy. 2010;40(5):811–9. https://doi.org/10.1111/j.1365-2222.2009.03437.x.
37. Zafar H, Saier MJ. Gut bacteroides species in health and disease. Gut Microbes. 2021;13(1):1–20. https://doi.org/10.1080/19490976.2020.1848158.
38. Qu R, Zhang Y, Ma Y, Zhou X, Sun L, Jiang C, Zhang Z, Fu W. Role of the gut microbiota and its metabolites in tumorigenesis or development of colorectal cancer. Adv Sci (Weinh). 2023;10(23):e2205563. https://doi.org/10.1002/advs.202205563.
39. Shin JH, Tillotson G, Mackenzie TN, Warren CA, Wexler HM, Goldstein E. Bacteroides and related species: the keystone taxa of the human gut microbiota. Anaerobe. 2024;85:102819. https://doi.org/10.1016/j.anaerobe.2024.102819.
40. Boleij A, Hechenbleikner EM, Goodwin AC, Badani R, Stein EM, Lazarev MG, Ellis B, Carroll KC, Albesiano E, Wick EC, et al. The bacteroides fragilis toxin gene is prevalent in the colon mucosa of colorectal cancer patients. Clin Infect Dis. 2015;60(2):208–15. https://doi.org/10.1093/cid/ciu787.
41. Dejea CM, Fathi P, Craig JM, Boleij A, Taddese R, Geis AL, Wu X, Destefano SC, Hechenbleikner EM, Huso DL, et al. Patients with familial adenomatous polyposis harbor colonic biofilms containing tumorigenic bacteria. Science. 2018;359(6375):592–7. https://doi.org/10.1126/science.aah3648.
42. Walker KA, Obrist MW, Mildiner-Earley S, Miller VL. Identification of ysrt and evidence that ysrrst constitute a unique phosphorelay system in yersinia enterocolitica. J Bacteriol. 2010;192(22):5887–97. https://doi.org/10.1128/JB.00745-10.
43. Kang D, Kirienko DR, Webster P, Fisher AL, Kirienko NV. Pyoverdine, a siderophore from *Pseudomonas aeruginosa*, translocates into *C. elegans*, removes iron, and activates a distinct host response. Virulence. 2018;9(1):804–17. https://doi.org/10.1080/21505594.2018.1449508.
44. Hoffman JA, Badger JL, Zhang Y, Huang SH, Kim KS. *Escherichia coli* k1 asla contributes to invasion of brain microvascular endothelial cells in vitro and in vivo. Infect Immun. 2000;68(9):5062–7. https://doi.org/10.1128/IAI.68.9.5062-5067.2000.
45. Bialek-Davenet S, Lavigne JP, Guyot K, Mayer N, Tournebize R, Brisse S, Leflon-Guibout V, Nicolas-Chanoine MH. Differential contribution of acrab and oqxab efflux pumps to multidrug resistance and virulence in *Klebsiella pneumoniae*. J Antimicrob Chemother. 2015;70(1):81–8. https://doi.org/10.1093/jac/dku340.
46. Nolivos S, Cayron J, Dedieu A, Page A, Delolme F, Lesterlin C. Role of acrab-tolc multidrug efflux pump in drug-resistance acquisition by plasmid transfer. Science. 2019;364(6442):778–82. https://doi.org/10.1126/science.aav6390.
47. Yekani M, Baghi HB, Naghili B, Vahed SZ, Soki J, Memar MY. To resist and persist: important factors in the pathogenesis of bacteroides fragilis. Microb Pathog. 2020;149:104506. https://doi.org/10.1016/j.micpath.2020.104506.
48. Patrick S. A tale of two habitats: *Bacteroides fragilis*, a lethal pathogen and resident in the human gastrointestinal microbiome. Microbiology (Reading). 2022. https://doi.org/10.1099/mic.0.001156.
49. Papaparaskevas J, Katsandri A, Pantazatou A, Stefanou I, Avlamis A, Legakis NJ, Tsakris A. Epidemiological characteristics of infections caused by *Bacteroides*, *Prevotella* and *Fusobacterium* species: a prospective

observational study. Anaerobe. 2011;17(3):113–7. https://doi.org/10.1016/j.anaerobe.2011.05.013.
50. Dickson RP, Singer BH, Newstead MW, Falkowski NR, Erb-Downward JR, Standiford TJ, Huffnagle GB. Enrichment of the lung microbiome with gut bacteria in sepsis and the acute respiratory distress syndrome. Nat Microbiol. 2016;1(10):16113. https://doi.org/10.1038/nmicrobiol.2016.113.
51. Dickson RP, Schultz MJ, van der Poll T, Schouten LR, Falkowski NR, Luth JE, Sjoding MW, Brown CA, Chanderraj R, Huffnagle GB, et al. Lung microbiota predict clinical outcomes in critically ill patients. Am J Respir Crit Care Med. 2020;201(5):555–63. https://doi.org/10.1164/rccm.201907-1487OC.
52. Tang J, Huang M. Genetic causal association between gut microbiota and sepsis: evidence from a two-sample bidirectional Mendelian randomization analysis. J Intens Med. 2024;4(3):362–7. https://doi.org/10.1016/j.jointm.2023.11.006.

Publisher's Note